Supplementary Material: Unraveling the Main Chain Effects of Fused Thiophene Conjugated Polymers in Electrochromism

Kaiwen Lin[1,#], Haoshen Liang[1,#], Yawen Zheng[1], Ronglin Hu[1], Hong Chen[2], Zhixin Wu[4], Xiaobin Zhang[1], Hui Xie[1], Yuehui Wang[1], Qinglin Jiang[3], Baoyang Lu[4]

[1]Department of Materials and Food, University of Electronic Science and Technology of China Zhongshan Institute, Zhongshan 528402, P.R. China

[2]School of Materials and Energy, University of Electronic Science and Technology of China, Chengdu 610054, P.R. China

[3]State Key Laboratory of Luminescent Materials and Devices, South China University of Technology, Guangzhou 510640, P.R. China

[4]Flexible Electronics Innovation Institute (FEII), Jiangxi Science and Technology Normal University, Nanchang 330000, P.R. China

[#]Authors contributed equally.

Correspondence to: Dr. Kaiwen Lin, Department of Materials and Food, University of Electronic Science and Technology of China Zhongshan Institute, Zhongshan 528402, P.R. China. E-mail: kevinlin1990@163.com; Prof. Yuehui Wang, Department of Materials and Food, University of Electronic Science and Technology of China Zhongshan Institute, Zhongshan 528402, P.R. China. E-mail: wyh@zsc.edu.cn; Prof. Qinglin Jiang, State Key Laboratory of Luminescent Materials and Devices, South China University of Technology, Guangzhou 510640, P.R. China. E-mail: jiangql@scut.edu.cn

EXPERIMENTAL

Instruments and characterization

^{1}H and ^{13}C NMR spectra were tested on a Bruker AV-500 with tetramethylsilane (TMS) as an internal reference. The geometry was optimized by density functional theory (DFT) calculations performed at the B3LYP/6-311G(d,p) level using the Gaussian 09. UV-vis spectra of the monomers dissolved in $CHCl_3$ were taken by using Perkin-Elmer Lambda 900 Ultraviolet-Visible Near-Infrared spectrophotometer. With an F-4500 fluorescence spectrophotometer (Hitachi), the fluorescence spectra of the monomers were determined. Scanning electron microscopy (SEM) images were obtained on a JEOL JSM-6700F scanning electron microscope.

Electropolymerization and electrochemical tests

All the electrochemical experiments and polymerization of monomers were performed in a one-compartment cell with the use of spectroelectrochemical workstation of Xi Pu Guang Dian (XP-SEC-BAC). For electrochemical tests, the working and counter electrodes were both Pt wires with a diameter of 1 mm, while the reference electrode (RE) was Ag/AgCl. The Ag/AgCl was prepared by chronoamperometry method at potential of 1.5 V for 100 s in hydrochloric acid (6 mol L^{-1}) and calibrated with the SCE system. Bu_4NPF_6 as electrolyte was dissolved in anhydrous CH_2Cl_2 (0.1 mol L^{-1}). All the solutions were distilled in a dry nitrogen stream before use. Polymer films were obtained by potentiodynamic regime. After polymerization, the films were washed repeatedly with anhydrous CH_3CN to remove the electrolyte and monomer.

Electrochromic study

Spectroelectrochemistry and kinetic studies of polymers were recorded on a spectroelectrochemical workstation of Xi Pu Guang Dian (XP-SEC-BAC). The spectroelectrochemical cell consisted of a quartz cell, an Ag/AgCl electrode as reference electrode, a Pt wire as counter electrode, and an indium tin oxide (ITO) coated glass as the transparent working electrode. All measurements were carried out in CH_3CN containing Bu_4NPF_6 (0.1 mol L^{-1}).

Spectroelectrochemical analyses were performed by recording the changes in the

absorption spectra using diverse voltage pulses. Under the applied potential, an electrochromic polymer will perform oxidation behavior with producing radical cations (polarons) and further oxidation produce dications (bipolarons), allowing new electronic transition thereby changing absorption spectra. Upon stepwise oxidation of the electrochromic polymers, the formation of polaron and bipolaron leads to new absorption bands at larger wavelength. Additionally, the CIE 1931 color coordinates (L* a* b*, where L* represents lightness, a* the red/green balance, and b* the yellow/blue balance) of the polymer film were determined in both its neutral and oxidized states.

The potentials were alternated between the reduced and oxidized states with a residence time of 2s, 5s, 10 s, and 20 s. The optical contrast at the specific wavelength (λ) was determined by ΔT% values of polymer films, using the following equation:

$$\Delta T = \left| T_{ox} - T_{red} \right|$$

The colouration efficiency (*CE*) is defined as the relation between the injected/ejected charge as a function of electrode area (Q_d) and the change in optical density (ΔOD) at the specific wavelength (λ) of the sample as illustrated by the following equation:

$$\Delta OD = \log(T_{ox}/\ T_{red})$$

$$CE = \Delta OD / Q_d$$

Flexible electrochromic devices (ECDs)

Flexible electrochromic devices were fabricated as device structure of indium tin oxide/polyethylene terephthalate (ITO/PET) /electrochromic active layer/gel electrolyte/ ITO/PET. The electrochromic layer was carried out via potentiostatic electrolysis of polymer films on flexible ITO/PET substrate and then the film was rinsed with CH_2Cl_2 to remove precursors, oligomers and the residual electrolyte. As a vital component of flexible ECDs, gel electrolyte displays unique advantages over liquid and solid electrolyte, such as no risk of leakage, high chemical stability and fast switching time. To prepare the gel electrolyte in this work, chemicals including Lithium perchlorate ($LiClO_4$, 1.35 g), CH_3CN (1.5 ml) and propylene carbonate (PC, 15 ml) were added in the flask. Then, polymethyl methacrylate (PMMA, 1.25 g) was slowly added in the mixture, followed by stirring of 12 h along with reflux condensation at

65 °C. The gel electrolyte was obtained with a composition of CH_3CN: PC: $LiClO_4$: PMMA (5.4 wt%: 82.7 wt%: 6.2 wt%: 5.7 wt%).

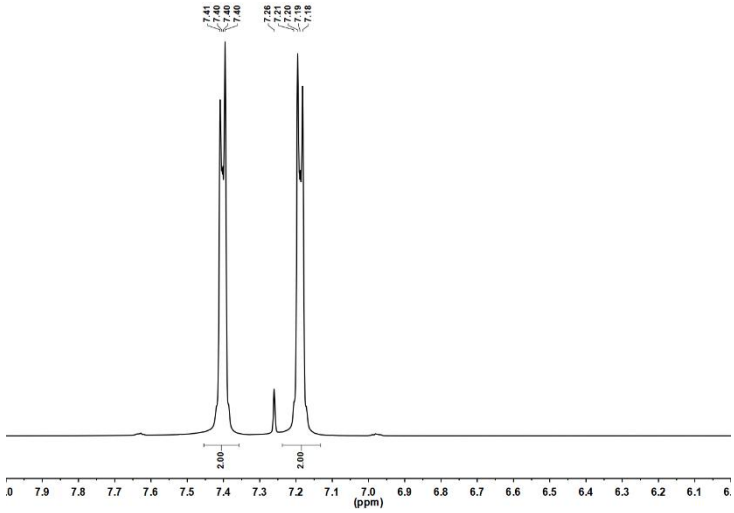

Supplementary Figure 1. ^1H NMR spectrum of T.

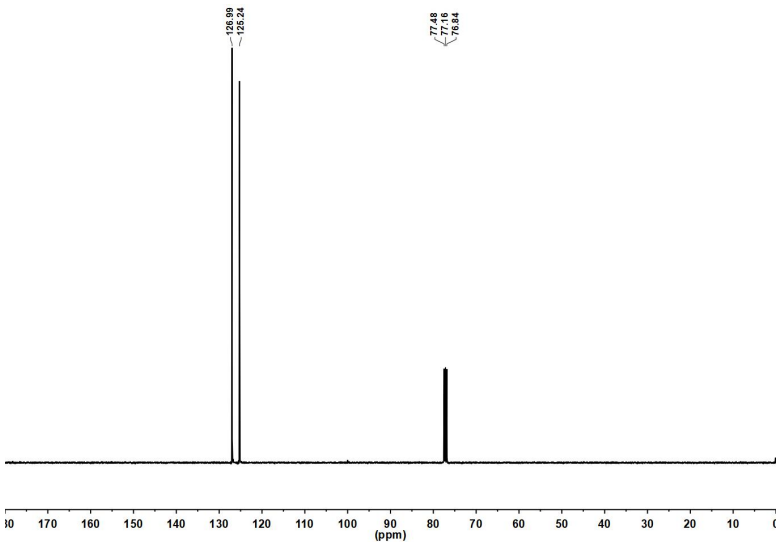

Supplementary Figure 2. ^{13}C NMR spectrum of T.

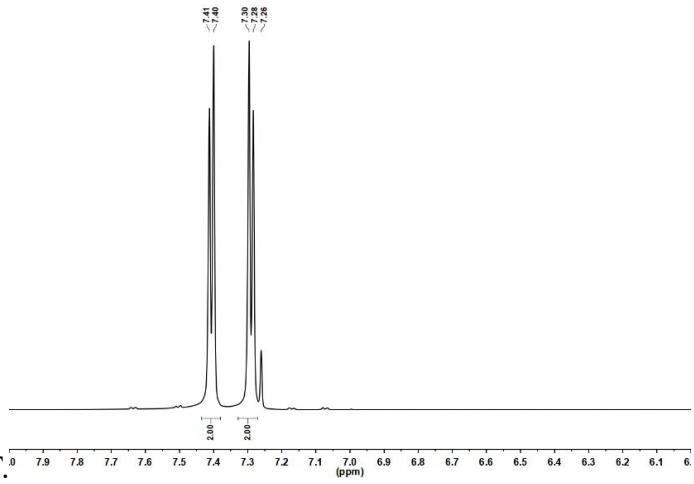

Supplementary Figure 3. ^{1}H NMR spectrum of TT.

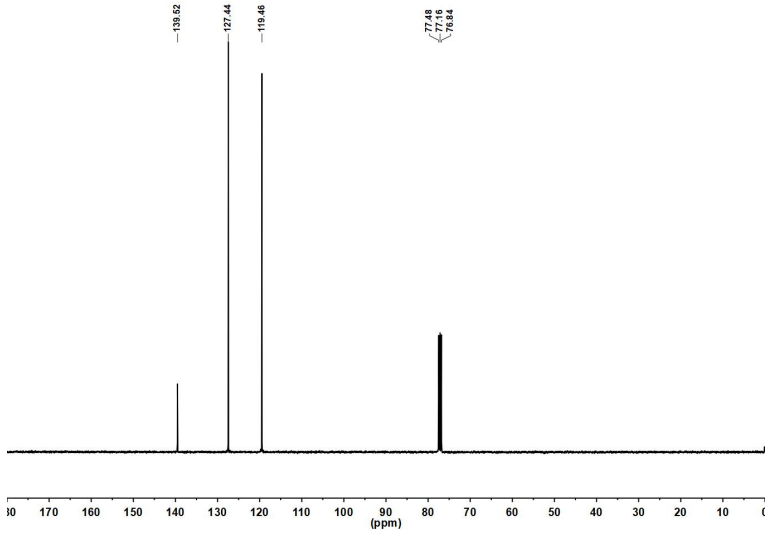

Supplementary Figure 4. ^{13}C NMR spectrum of TT.

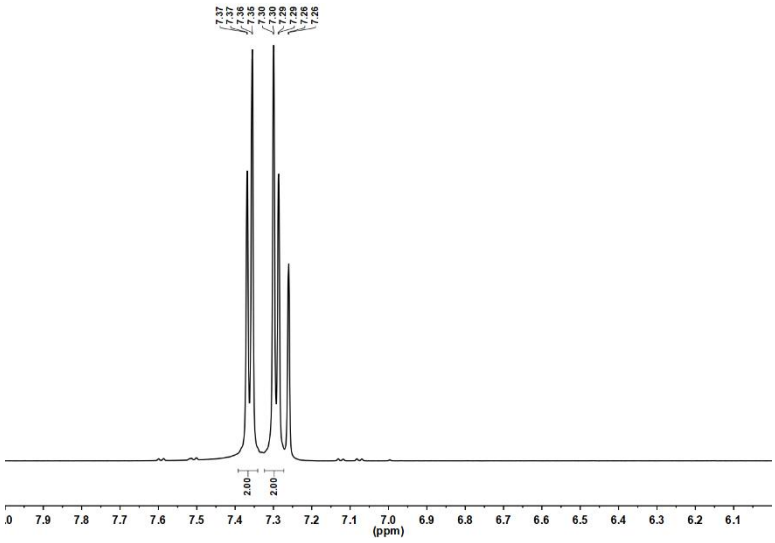

Supplementary Figure 5. ^{1}H NMR spectrum of DTT.

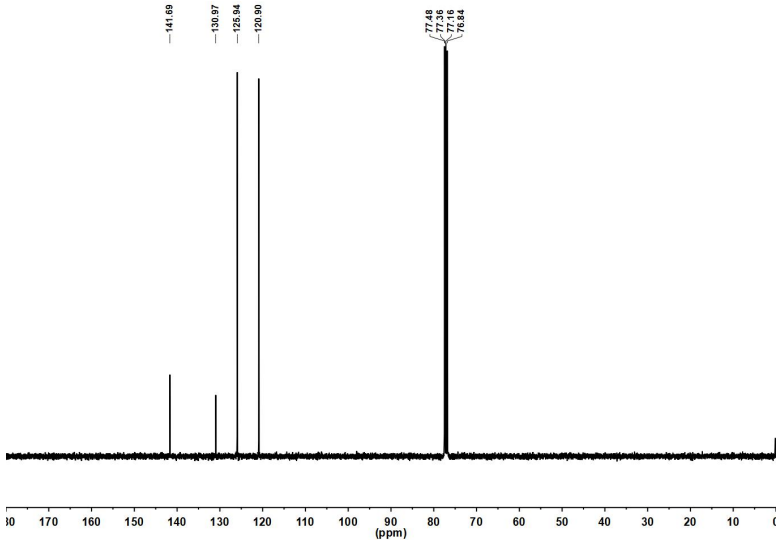

Supplementary Figure 6. ^{13}C NMR spectrum of DTT.

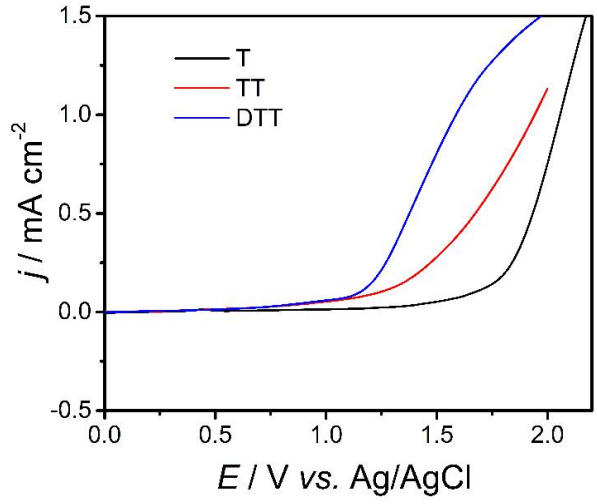

Supplementary Figure 7. Anodic polarization curves of 0.01 mol L^{-1} T, TT, and DTT in CH_2Cl_2-Bu_4NPF_6 (0.1 mol L^{-1}). Potential scan rate: 100 mV s^{-1}.

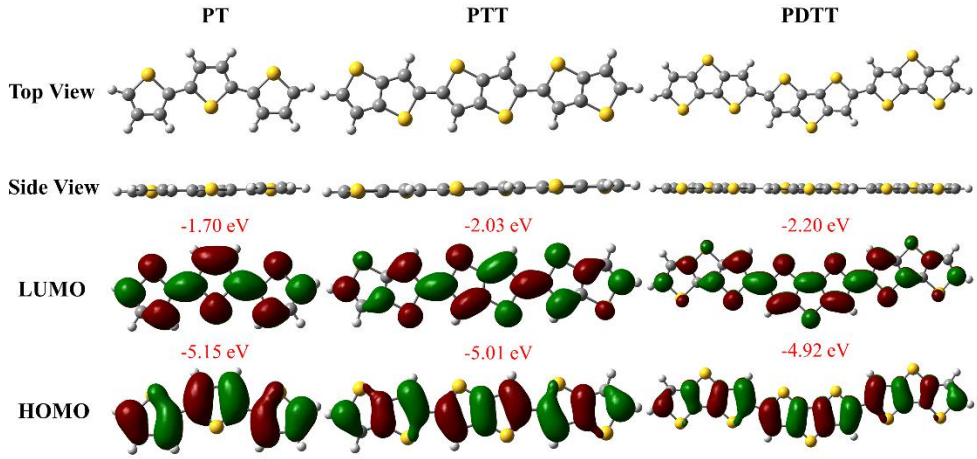

Supplementary Figure 8. Optimized molecular geometries and frontier molecular orbital distributions of PT, PTT, and PDTT (with 3 repeat units) using density functional theory (DFT) by Gaussian 09 at B3LYP/6-31G(d,p) level.

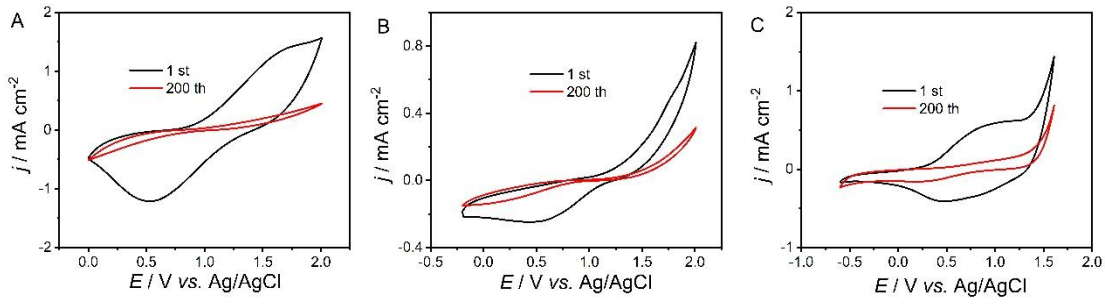

Supplementary Figure 9. Redox stability of PT (A), PTT (B), and PDTT (C) film with a scan rate of 200 mV s^{-1} in CH_2Cl_2-Bu_4NPF_6 (0.1 mol L^{-1}).

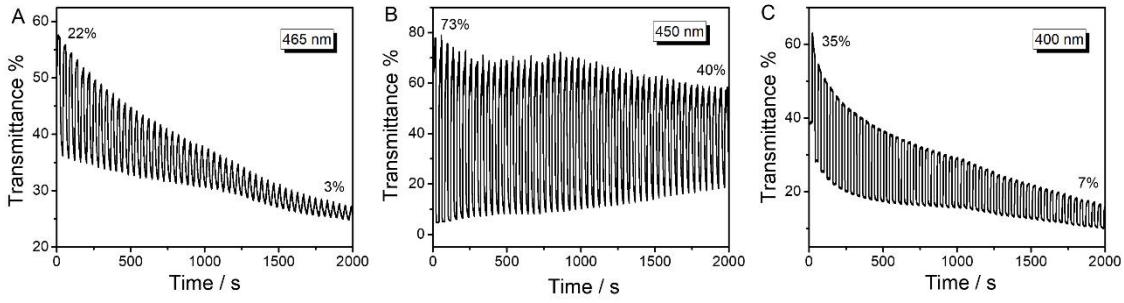

Supplementary Figure 10. Long-term stability tests of PT (A), PTT (B), and PDTT (C) monitored at 465 nm, 450 nm and 400 nm with the intervals of 20 s, respectively.

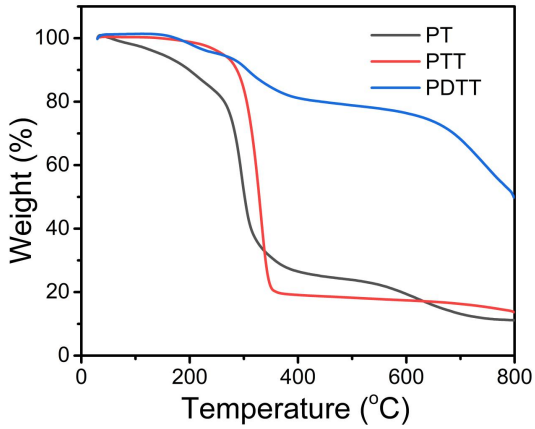

Supplementary Figure 11. Thermogravimetric analysis (TGA) curves of PT, PTT, and PDTT.